CHAPTER II

THEORETICAL BACKGROUND

The tremendous growth of the plastics industry during the last three decades has effected a significant increase in plastics disposal [3]. Municipal Solid Waste (MSW) generation grew from 88 million tons (2.68 lbs./person/day) in 1960 to 214 million tons (4.51 lbs./person/day) in 1994. In 1996, the waste generation decreased to 210 million pounds (4.33 lbs./person/day) shown in Figure 2.1 [4].

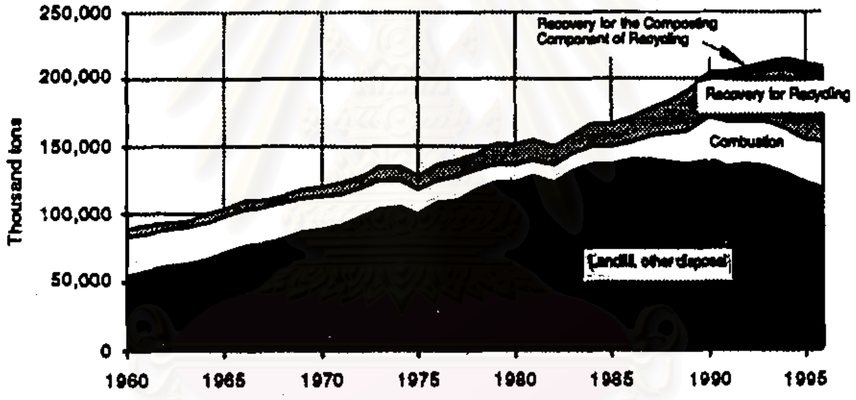

Figure 2.1 Municipal Solid Waste (MSW) management, 1960-1996 [4]

The growth of plastics in MSW is shown in Figure 2.2. Plastic products had generated the largest increase for all materials by nearly 1 million tons from 1995 to 1996 in MSW generation. The recovery of MSW was very small various plastic resins in the municipal solid waste are given in Table 2.1.

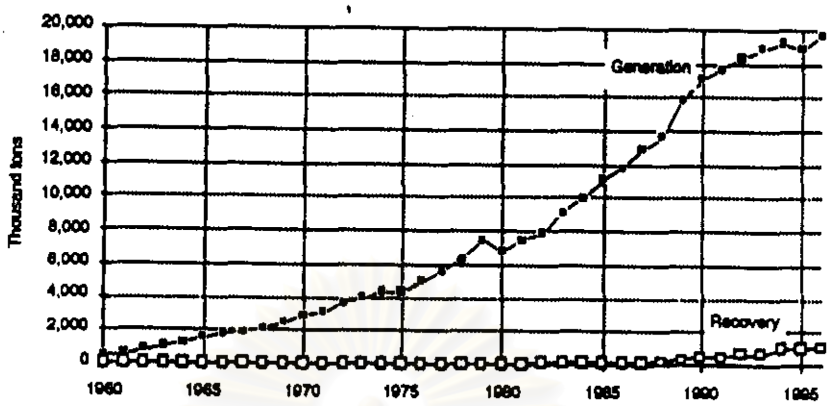

Figure 2.2 Plastics waste generation and recovery during 1990-1996[4]

Table 2.1 Plastics resin in MSW in 1996 (in thousands of tons) [4]

Resin[a]	MSW generation	Recovered for recycling
PET	1,700	350
HDPE	4,120	410
PVC	1,230	Negligible
LDPE/LLDPE	5,010	110
PP	2,580	130
PS	1,990	30
Other resins	3,130	30
Total plastics in MSW	19,760	1,060 (5.4%)

[a] PET = polyethylene terephthalate; HDPE = high-density polyethylene; PVC = poly(vinyl chloride); LDPE/LLDPE = low-density polyethylene/linear low-density polyethylene; PP = polypropylene; PS = polystyrene.

Source: Ref. 1.

2.1 Recycled Plastic and Quality

At high temperature curing the transforming process, plastic will be melted into a liquid form and once the temperature is released, the plastics cools off and then transforms into a solid form in accordance with the shape of its mold. Unless plastic molecules remained unchanged after the transforming process, the quality of plastic products would remain the same. However, the transforming process to produce products such as bottles, plastics bags, ropes, auto parts and electrical parts will in fact affect the structure of molecules as the chain of the molecules will be cut short or changed due to the reaction with oxygen or with other chemicals [5]. Especially, they react with oxygen due to a lot of oxygen in air. So, the structure of molecules degraded fastly. The reaction with heat, mechanical force (compression), and oxygen are formed into some functional groups [6].

A typical mechanistic scheme for the oxidation of polymer systems is displayed in Figure 2.3. This scheme originates from work on the combustion of liquid hydrocarbons and is often referred to as the Bolland-Gee mechanism. Here, a macroradical is formed initially which will then react with oxygen to form a peroxy radical. The peroxy radicals are reactive and will abstract a hydrogen atom either by an intra or intermolecular process to generate a hydroperoxide group and another macroradical site. The hydroperoxides will then decompose resulting in the formation of alkoxy and hydroxy radicals. Chain transfer reactions will then take place resulting in further accelerated hydrogen atom abstraction reactions giving rise to more free radical species and the whole process becomes autocatalytic[6].

Initiation

$$\text{POLYMER} \longrightarrow \text{P}\cdot \qquad (2.1)$$

$$\text{P}\cdot + \text{O}_2 \longrightarrow \text{PO}_2\cdot \qquad (2.2)$$

$$\text{PO}_2\cdot + \text{PH} \longrightarrow \text{PO}_2\text{H} + \text{P}\cdot \qquad (2.3)$$

Chain Branching

$$2\text{PO}_2\text{H} \longrightarrow \text{PO}\cdot + \text{PO}_2\cdot + \text{H}_2\text{O} \qquad (2.4)$$

$$\text{PO}_2\text{H} \longrightarrow \text{PO}\cdot + \cdot\text{OH} \qquad (2.5)$$

$$\text{PH} + \cdot\text{OH} \longrightarrow \text{P}\cdot + \text{H}_2\text{O} \qquad (2.6)$$

Termination

$$2\,PO_2\cdot \longrightarrow \text{Inert products} \tag{2.7}$$

$$PO_2\cdot + P\cdot \longrightarrow PO_2P \tag{2.8}$$

$$2\,P\cdot \longrightarrow P\text{-}P \tag{2.9}$$

Figure 2.3 Bolland-Gee mechanism [7]

The reaction of PE with heat, mechanical force (compression), and oxygen are formed into some functional groups (especially, the hydroperoxide group; ROOH) in Figure 2.4. The functional group can mainly be formed in a production of plastic products [6].

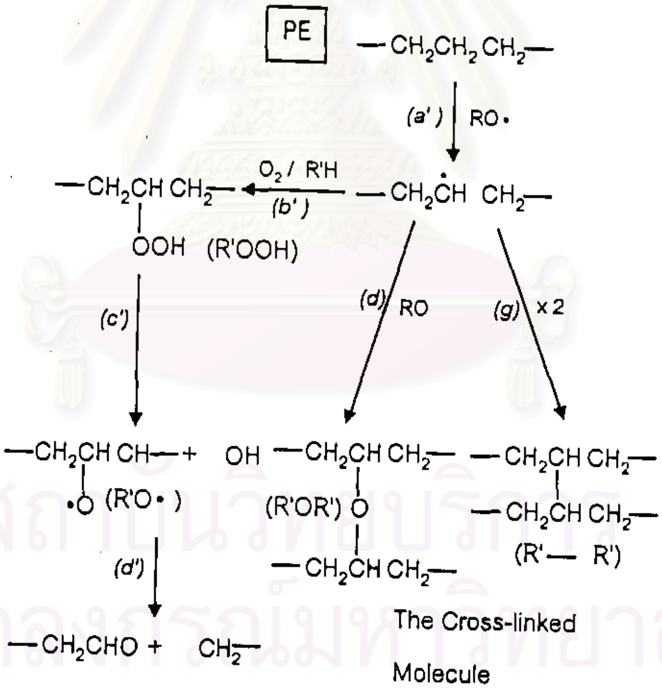

Figure 2.4 The degradation reaction of PE [6]

Melt plastic is normally, in a machine, it receives the limited oxygen. For PE, it induces cross-linking between molecules and gel formation. They affect melt flow index (MFI) in a decreasing manner shown in Figure 2.5 [6].

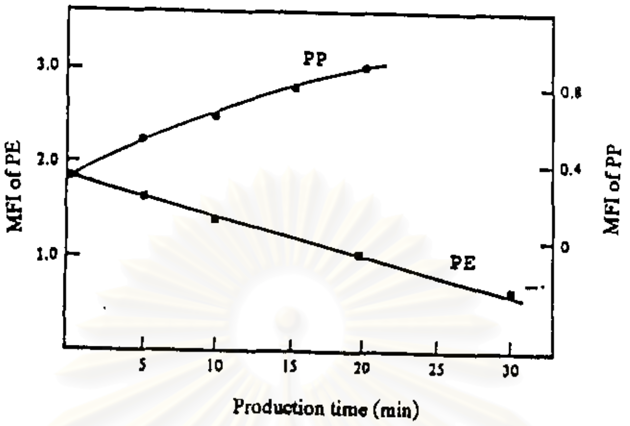

Figure 2.5 Degradation of PE and PP expressed as MFI during processing [6]

However, The chain scission effects to bad a mechanical property. Besides, the degradation in a production of plastic product effects to quality of plastic and service time of the product at outdoors or UV, or sun-light exposure [6]. As a result, the quality of the plastics will be physically and negatively changed [5]. Some plastic causes cross-linkings between molecules. Normally plastics is stronger but rigid. The molecular weight and mechanical strength are decreased, or some molecular structures are changed [6]. For example the tensile strength and impact strength become lower and the color is also darker [5].

The degradation of plastic depends on:

1. Kind of plastic material.
2. Product processing temperature.
3. Time period for melt plastic state or number of plastic extrusion time.
4. Oxygen content by the plastic intake [6].

To prevent the structure of plastic from being damaged and to increase the quality of recycled plastics after transforming. The key factors causing the negative changes are as follows:

1. Declined quality of plastic resin stabilizer,
2. Physical damages by cutting or crushing,
3. UV sun light effect or exposure condition before recycling,
4. Dirt or foreign substances mixed with plastic during the transforming process:
    - 4.1 Pigments when compounding,
    - 4.2 Some chemical additives,
    - 4.3 Moisture,
    - 4.4 Mixture of different kinds of plastic.
5. Overheating in the transforming process [5].

2.2 A Processing System for Waste Plastics

The elements of a processing system to recycle plastics separated from urban refuse would consist of a group of unit operations of the type used in minerals processing, selected from a variety of methods to accommodate the variability of waste content. On the basis of information obtained from literature on the properties of virgin plastics has been designed with the flow diagram shown in Figure 2.6 [8].

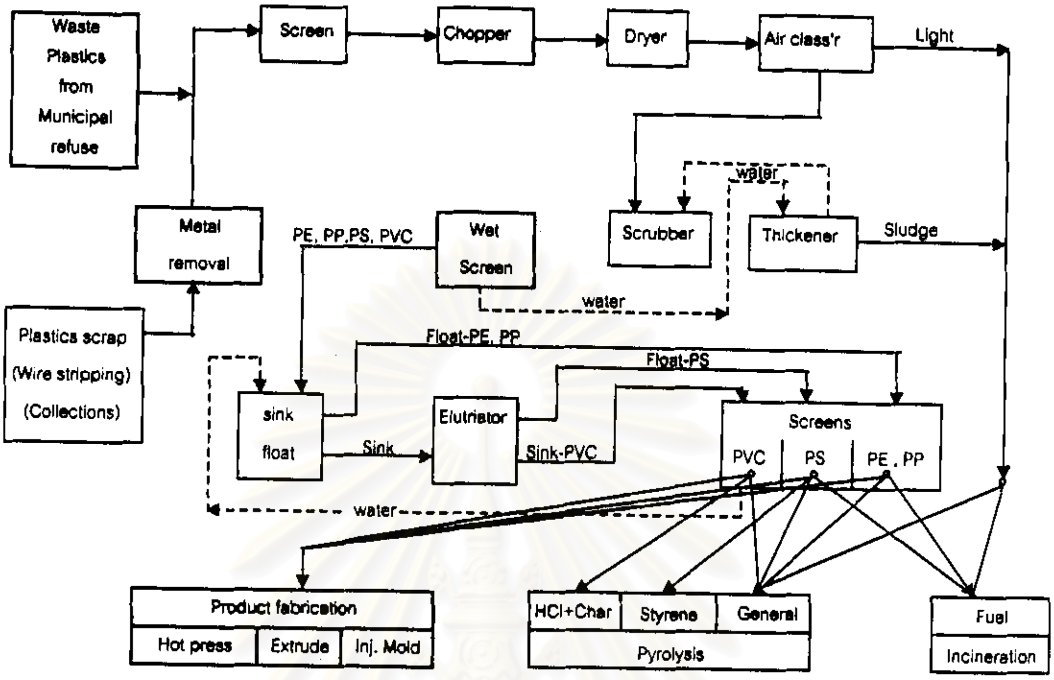

Figure 2.6 Proposed flow diagram of a processing system for reclaiming waste plastics [8]

2.3 HDPE Recycling

About 145 million pounds of HDPE have been identified as being recycled in 1989. This represented a significant increase of over 55% from the approximately 93 million pounds in 1988. Many communities are beginning to collect milk jugs and water jugs and detergent containers for HDPE recycling. The growth in HDPE recycling is presented in Figure 2.7 [9].

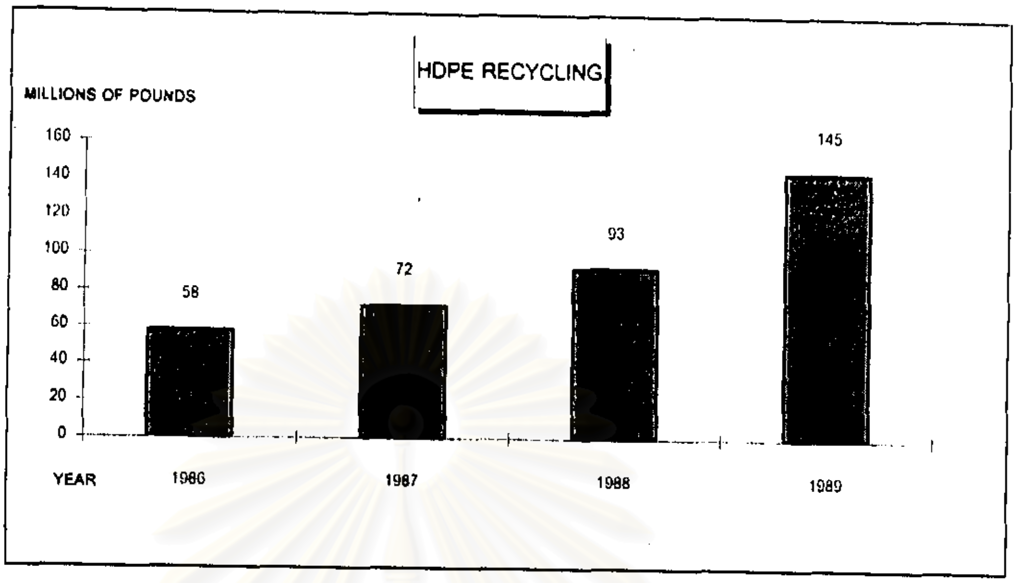

Figure 2.7 HDPE Recycling [9]

2.3.1 Characteristics of Recycled HDPE

The advantages of recycled HDPE from milk and juice bottles are: (i) their highly recognizable form and their abundant supply, (ii) the resultant recycled product has consistent MFI and density from lot-to-lot over time, since dairy resin is a tightly specified blow moulding resin, and (iii) recycling of HDPE milk containers can potentially give a clean, natural-coloured product. Furthermore, the resultant recyclate has essentially the same rheological properties as the virgin resin, since it does not undergo any appreciable thermal degradation during recycling [10].

There are also, however, a number of barriers to limit the widespread use of dairy post consumer recycled (PCR). These include: (i) dairy resin is a fractional MFI material (i.e. 0.6 g/10 min) and has been tailored for blow moulding in milk and juice bottles; (ii) because of its high molecular weight, it does not produce economical cycle times when injection moulded; (iii) the dairy resin is a homopolymer and does not possess adequate environmental stress crack resistance (ESCR) properties for recycling into detergent or bleach bottles; (iv) occasional colour variation due to caps and shampoo bottles also makes it unsuitable for a lightly pigmented application; and (v) it has been found that injection mouldings produced from blends containing recycled HDPE milk bottle resin exhibit considerably greater shrinkage than do mouldings from the neat HDPE injection moulding resin [10].

2.4 LDPE Recycling

LDPE recycling is widespread, although not to the same magnitude as HDPE recycling. The majority of LDPE, which is recycled originates from post-industrial scrap and there is only a limited proportion of recycled LDPE which can be regarded as post-consumer recyclate [10].

2.5 Melt Blending Process

Different polymers when blended together may be miscible, partially miscible, or completely immiscible. General classification of polymer blends are given in Figure 2.7. The methods of blending may be by polymerization blending, latex blending, fine powder mixing, and melt blending. The melt blending is employed in our present, which was simply by melting polymers together while blending [11].

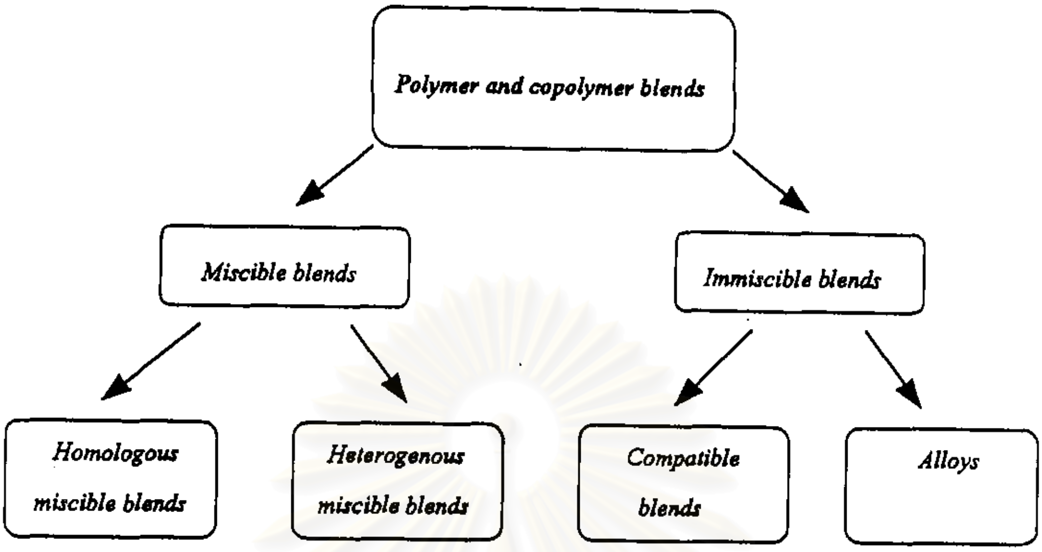

Figure 2.8 Classification of polymer blends [11]

Thermodynamic consideration predicts the temperature and concentration at which phase separation occurs under equilibrium condition. Rheological properties of polymer melts affect the conditions of phase separation. The system with low interfacial tension tends to form compatible blends, examples of these are polyolefin blends such as PE/PP and LDPE/HDPE. Polymer pair with high interfacial tensions, such as PE/PS, will benefit considerably from compatibilization [11].

During melt processing, droplets of polymer are deformed by hydrodynamic forces leading to elongated and distorted structures. When the mixing process is stopped, e.g. when the polymer melt exits in an extruder, the system is driven thermodynamically to reduce the interfacial tension of the blend by lowering the surface area between the two phases. This process involves motion of the liquid polymers until solidification occurs. As no external forces are driving the process, it is said to be a spontaneous change, full minimisation of the interfacial area does not occur, since the density difference between the two phases is low, and the viscosities are high. The effect upon morphology is that the elongated structures tend to form spheres, or in the case of co-continuous morphologies a coalescing of the structure followed by the formation of large spherical particles. The implications of these are (a) control of the blend system by choice of components and mixing conditions will be hampered by the spontaneous morphological changes that occur after the mixing process has finished, and (b) determination of the effect of mixing conditions upon morphology by analysis of the final article is limited by the spontaneous morphological changes occurred upon cessation of the mixing [11].

2.6 Two Dimensional Process

2.6.1 Blown Film Extrusion Process

By definition, the term film is used for material less than 0.010-in. thick and sheet for that which is thicker. Biaxial orientation often can be achieved in a blown-film extrusion. The molten polymer (Figure 2.9) is extruded through a ring-shaped die around a mandrel. The tube or sleeve so formed is expanded around an air bubble, is cooled to below T_g and then is rolled into a flattened tube and wound up. Since the bubble is sealed at one end by the mandrel, and at the other by the nip where the tube is flattened, air cannot escape and the bubble acts like a permanent shaping mandrel once it has been injected. Cooling of the film is controlled by an air ring below the bubble. When polyethylene is cool, the crystalline material is cloudy compared with the clear amorphous melt, so the transition line which coincides with dimensional stabilization is called the frost line. The blow up ratio may range as high as 4 or 5, although 2.5 might be a more typical figure. Orientation occurs in the hoop direction during blow up.

Orientation in the machine direction (in the direction of extrudate flow from the die) can be induced by tension from the nip roll [12].

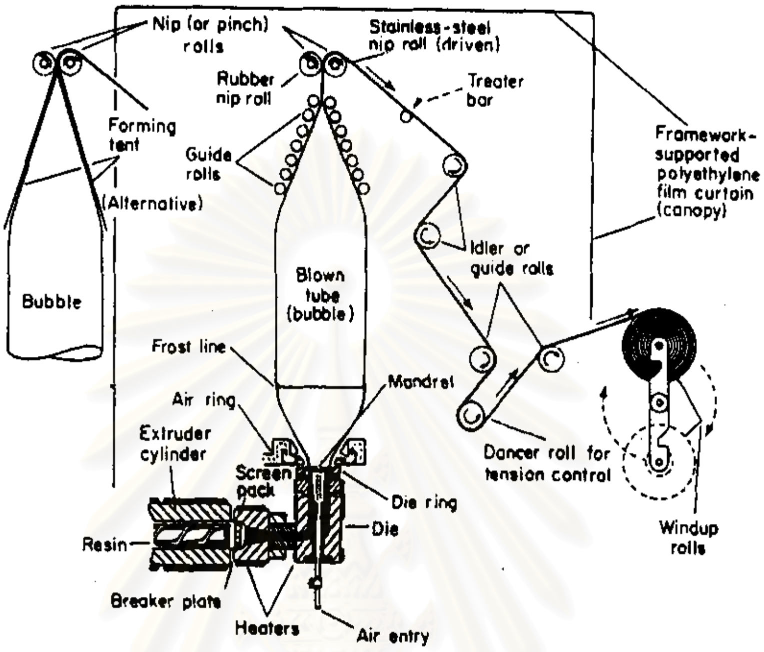

Figure 2.9 Schematic drawing of chill-roll film extrusion equipment [12]

2.6.2 The Influences for Blown Film Process and Properties

The blown film extrusion process is used extensively to fabricate thermoplastic polymer into thin films. The film obtained from the blown film processes is known to be influenced by many variables (Figure 2.10). The intrinsic properties of the polymer have been related to film properties. But the same polymer, run on different equipment and at different conditions, will result in a variation of film properties. Many of these variables have been shown to have significant impact on film properties such as dart impact, tear strength, tensile properties, and optical properties. The influence of each of these variables on film properties has been found to be highly interactive with other variables [13].

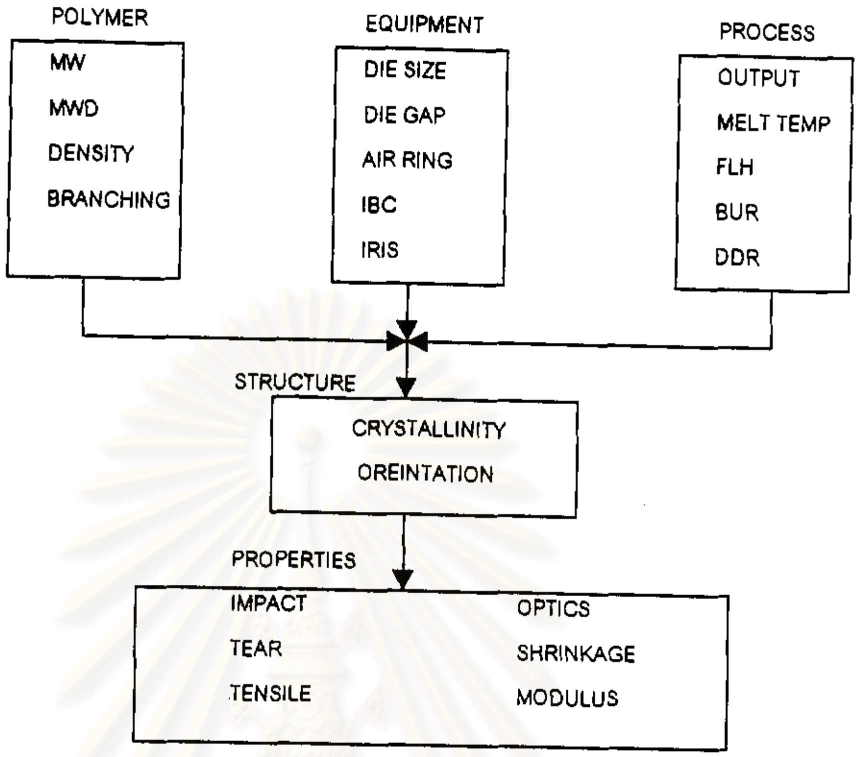

Figure 2.10 Blown film properties [13]

2.7 Mechanical Properties of HDPE and Recycled HDPE

Many polymer properties such as solvent, chemical, and electrical resistance and gas permeability are important in determining the use of a specific polymer in a specific application. However, the prime consideration in determining the general utility of a polymer is its mechanical behavior, that is, its deformation and flow characteristics under stress. The mechanical behavior of a polymer can be characterized by its stress-strain properties. This often involves observing the behavior of a polymer as one applies tension stress to it in order to elongate (strain) it to the point where it ruptures (pulls apart) [14].

Polymers vary widely in their mechanical behavior depending on the degree of crystallinity, degree of crosslinking, and the values of T_g and T_m. High strength and low extensibility are obtained in polymers by having various combinations of high degrees of crystallinity, or crosslinking, or rigid chains (characterized by high T_g). High extensibility and low strength in polymers are synonymous with low degrees of crystallinity and crosslinking and low T_g values. The temperature limits of utility of a polymer are governed by its T_g and/or T_m. Strength is lost at, or, near T_g for an amorphous polymer and at or near T_m for a crystalline polymer [14].

2.7.1 Dynamic Mechanical Properties of Polymers

Dynamic mechanical analysis (DMA) measures transition temperatures, flexural modulus, damping (energy dissipation), stress relaxation and creep characteristics of materials. DMA results can be correlated with other end-use properties such as vibration and acoustical damping, toughness and impact resistance. DMA results can be used to determine the compatibility of polymer blends and the effect of varying plastic/filler ratios [15].

Dynamic mechanical properties are the mechanical properties of materials as they are deformed under periodic forces. When a sinusoidal stress is applied to a perfectly elastic solid, the deformation, and hence the strain, occurs exactly in phase with the stress. A completely viscous material will respond with the deformation lagging 90° behind the applied stress. Polymeric materials usually exhibit viscoelastic behaviour which combine liquid-like and solid-like characteristics. When they are subjected to sinusoidally oscillating stress, the resulting strain is neither exactly in phase with the stress nor 90° out of phase, but is lagged behind the stress by some angles where $\delta < 90^\circ$. Figure 2.11 illustrates the relationship between stress, strain and time of viscoelastic materials which are subjected to sinusoidal oscillations. The magnitude of the loss angle is dependent upon the amount of internal motion occuring in same frequency range as the imposed stress [16].

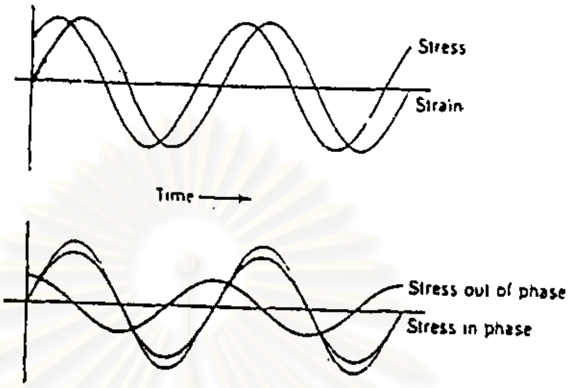

Figure 2.11 Phase difference between the stress and the strain [16]

For linear viscoelastic behaviour, the stress (σ) and strain (ε) can be expressed as follows:

$$\sigma = \sigma_0 \sin \omega t \tag{2.10}$$

$$\varepsilon = \varepsilon_0 \sin (\omega t-\delta) \tag{2.11}$$

Where σ_0 = maximum stress, ε_0 = maximum strain, ω = angular frequency, and δ = phase angle.

For viscoelastic materials, it is not sufficient to define modulus as the stress-strain ratio since this ratio varies between $-\alpha$ and $+\alpha$ depending on the time of measurement. Neither is it sufficient to define modulus as the ratio of maximum stress to maximum strain since this give no information about the phase difference. In general, a complex modulus (E*) is often defined for describing the dynamic mechanical properties of polymer since it can define both modulus and the phase difference.

$$E^* = E' + iE'' \tag{2.12}$$

$$E^* = [(E')^2 + (E'')^2]^{1/2} \tag{2.13}$$

E′ is the ratio of the amplitude of the in-phase component of stress to the strain amplitude and E″ is the ratio of the amplitude of the out-of-phase stress component to the strain amplitude. The relationships are:

$$E' = \frac{\sigma_0 \cos \delta}{\varepsilon_0} \tag{2.14}$$

$$E'' = \frac{\sigma_0 \sin \delta}{\varepsilon_0} \tag{2.15}$$

On the other hand, E′ is the in-phase (real) component of the complex modulus and usually known as the dynamic storage modulus which provides a measure of energy stored and recovered in cyclic deformation. E″ is the out-of-phase (imaginary) component of the complex modulus and usually known as the loss modulus. E″ is a measure of the energy dissipated as heat.

In addition, the ratio of the loss modulus to the storage modulus is very important quantity for specifying the dynamic mechanical properties of polymeric materials since it gives information about the phase difference between the two modulus components.

$$\tan \delta = E''/E' \tag{2.16}$$

This term is usually known as the loss factor. The loss tangent (tan δ), called internal friction or camping, is the ratio of energy dissipated per cycle to the maximum potential energy stored during a cycle [16].

2.7.2 Rheological Properties of HDPE and Recycled HDPE

The simplest and most ubiquitous type of melt rheometer is the capillary rheometer. While it is not very versatile in its capabilities, its popularity makes it important for the practitioner to understand its proper use and limitations. Capillary rheometers are used primarily to determine the viscosity in the shear rate range of 5 to 1,000 /s, although very long capillaries have occasionally been used to extend the range to much lower shear rates [17].

2.7.2.1 Apparent Shear Viscosity from Capillary Rheometer [18]

The derivation of the Poiseuille law for capillary flow will be found in most standard text on vicometry and yields

Wall shear stress, $$\sigma_s = \frac{PR}{2L} \qquad (\mathrm{N/m^2}) \qquad (2.17)$$

Wall shear rate, $$\dot{\gamma} = \frac{4Q}{\pi R^3} \qquad (\mathrm{/s}) \qquad (2.18)$$

Where P = the pressure drop ($\mathrm{N/m^2}$), Q = the volume flow rate ($\mathrm{m^3/s}$), R = the capillary radius (m), and L = the capillary length (m). By the selection of appropriate equipment it is possible conveniently to measure shear stresses in the range 10^3-10^6 $\mathrm{N/m^2}$ and shear rates in the range 0.001 to 500,000 /s.

Two modes of operation have been used: controlled pressure by dead weight loading or gas pressure (requiring a measurement of the volumetric flow rate), and controlled volume displacement (requiring a measurement of pressure) (Figure 2.12).

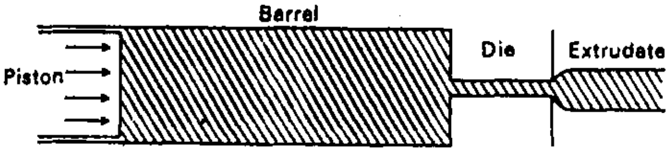

Figure 2.12 Capillary extrusion rheometer [18]

2.8 Morphology of HDPE and Recycled HDPE

Some methods are used to characterise the microstructure of polymer [18]. For convenience, as shown in Table 2.2, the microscopic methods can be divided into three categories: optical or light microscopy (OM), scanning electron microscopy (SEM), and transmission electron microscopy (TEM). In most cases some mode of sample preparation has to be used: viz. staining, swelling, fracturing or etching [20].

Table 2.2 Microscopic Methods.

No.	Parameter	Units	Optical Microscopy (OM)	Scanning Microscopy (SEM)	Transmission Microscopy (TEM)
1	Magnification	(time) ×	1 to 500	10 to 10^5	10^2 to 5.10^6
2	Resolution	nm	500 to 1000	5 to 10	0.1 to 0.2
3	Dimensionality	--	2 to 3	3	2
4	Field depth	µm	~ 1 (at high magn.)	10 to 100	~1
5	Field size	µm	10^3 to 10^5	1 to 10^4	0.1 to 100
6	Specimen	--	solid or liquid	solid	solid

Note: No. 1 total range of available magnification within each category;
No. 2 finest detail the microscope can resolve;
No. 3 nearly planar vision (2 dimensions) in TEM and at high resolution OM;
No. 4 ability to discern details perpendicular to the field direction;
No. 5 the diagonal size of field under observation;
No. 6 only OM allows observation of liquid/liquid phase changes.

2.8.1 Light Microscopy or Optical Microscopy

Light microscopy is one of the most important techniques in the study of polymer, as it is relatively simple and cheap and the specimen preparation is not too complicated. However, the resolution of a light microscope is limited by the wavelength of visible light and by the quality of the objective lens.

The principle of a light microscope is shown diagrammatically in Figure 2.13 [19].

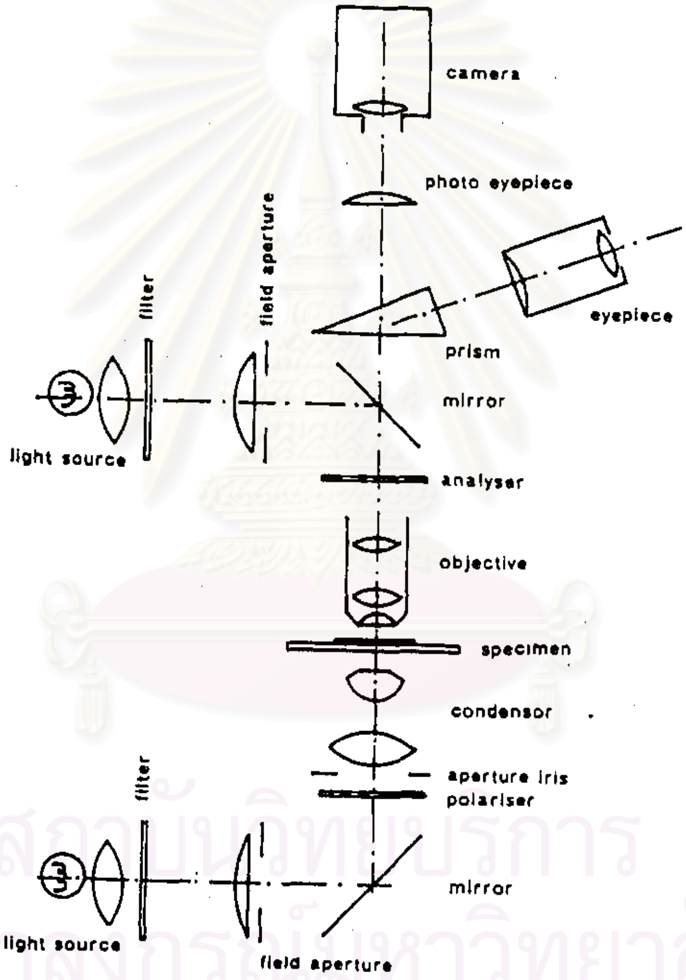

Figure 2.13 Schematic diagram of a light microscope [19].

2.8.2 Scanning Electron Microscopy

The advantages of scanning electron microscopy (SEM) are a good depth of field, good resolution and easy specimen preparation. The cost of the instrument is also less than the cost of a transmission electron microscope (TEM). However, only information on surface topography can be obtained and contrast is usually not suitable for good image processing. These two disadvantages do not outweigh the advantages and the technique is very popular.

The principle of an SEM (Figure 2.14) is shown as follows [19]:

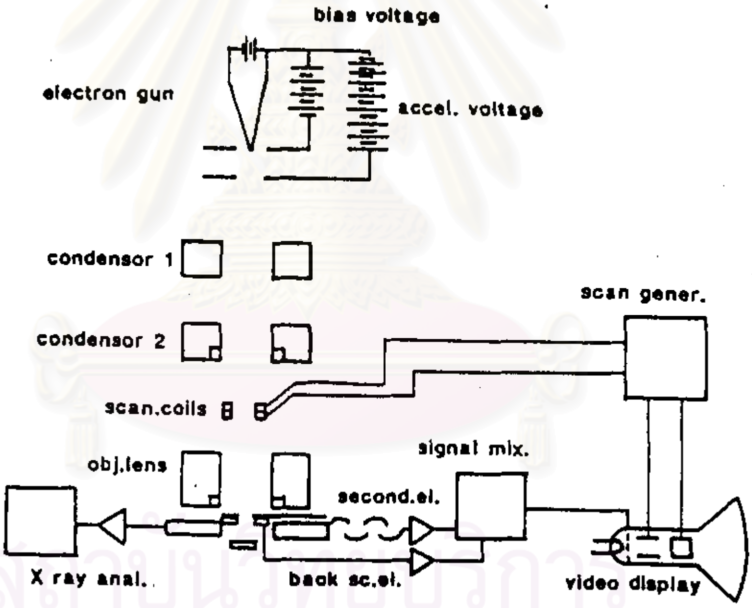

Figure 2.14 Schematic diagram of a scanning electron microscope [19]

2.8.3 Transmission Electron Microscopy

Transmission electron microscopy (TEM) represents the ultimate technique in terms of resolution and analysis of materials. It is the only technique, which provides information on the fine structure of materials down to atomic or molecular levels and elemental analysis from small volumes.

The principle of a TEM (Figure 2.15) is shown as follows [19]:

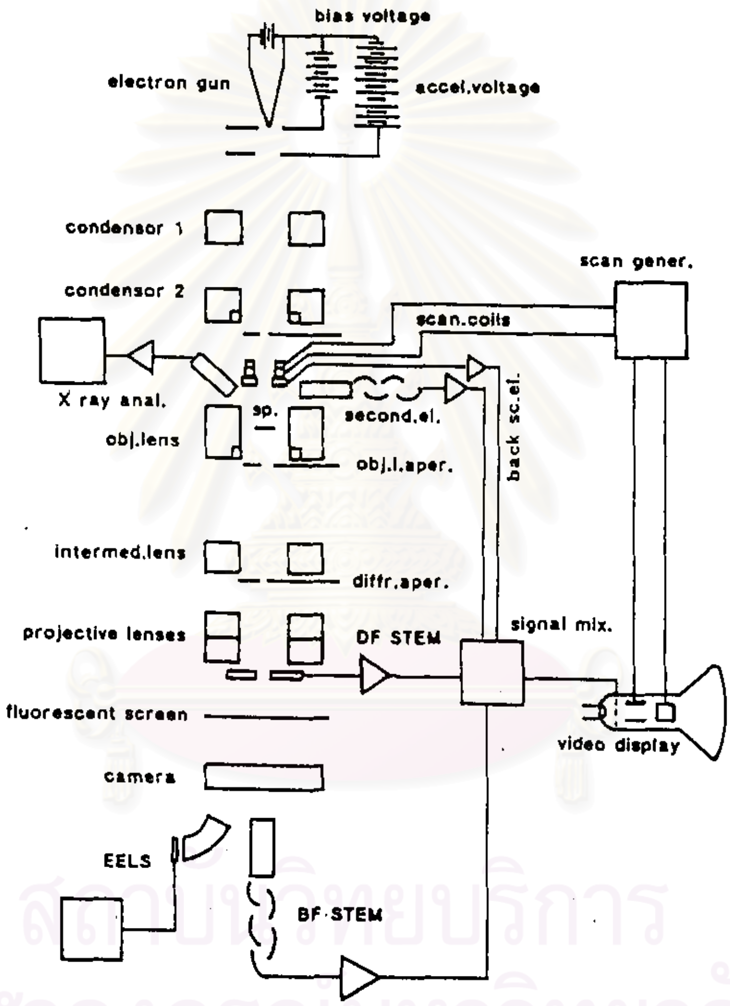

Figure 2.15 Schematic diagram of a transmission electron microscope with scanning and analytical facilities [19].

2.9 Thermal Properties of HDPE and Recycled HDPE

Differential scanning calorimeter (DSC) measures the heat flow into or out of a sample, which provides valuable data on crystallization rate, percent crystallinity, glass transition temperature, melting points, and specific heat. DSC can determine the oxidative stability of a material and analyze pressure-sensitive reactions [15].

2.9.1 Melting Point

The melting point of a sample is easily determined from a DSC scan. Knowledge of a plastic's melting point is useful for determination of optimum processing conditions. If the material processed at a temperature well above its melting point will be too fluid, resulting in ridges on the molded parts and some decomposition. A thermoplastic not heated to its melting point before molding will not fill the mold completely, causing cracks and stress points in the part.

The onset temperature of the melting peak and the peak maximum temperature are used to define the melting range of the polymer. Knowledge of both of these values is important to the process engineer because it gives him the temperature range within which the infection molding equipment must be operated.

The area under the melting peak is the heat required to melt a specific mass of the polymer. This heat of melting must be known to do the proper heat flow calculations, which are critical for the design of thermoplastics processing equipment.

Figure 2.16 shows the onset and peak temperatures for the melting of a polyethylene sample. The amount of heat (158 J/g) required to melt the polymer is a relative measure of the polymer's crystallinity.

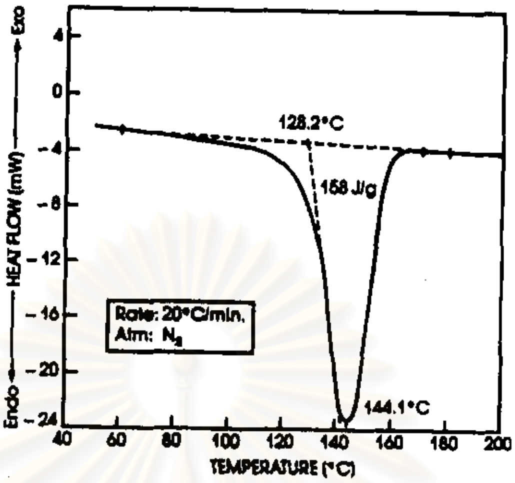

Figure 2.16 DSC of a high-density polyethylene melt [15]

2.10 X-ray Diffraction Analysis

2.10.1 Properties of X-rays

X-rays are generated when high-energy electrons impinge on a metal target (iron, copper, or molybdenum). The X-ray beam possesses a spectrum as shown in Figure 2.17 [16].

The X-ray spectrum consists of two parts:

i) A broad band responsible for the continuous radiation.

ii) Characteristic lines, called K_{α} and K_{β}. The K_{α} line is composed from two components K_{α_1} and K_{α_2}, separated by a very small wavelength interval.

K_{α} and K_{β} lines can be separated by absorbing filters made from metals such as zircon, nickel, or manganese (Table 2.3). Nickel-filtered CuK_{α} radiation (1.54178 A°) is the most useful X-ray radiation for polymer studies[16].

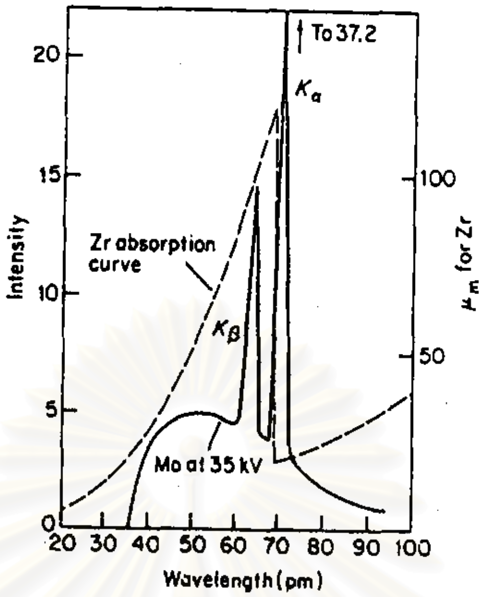

Figure 2.17 Zirconium absorption curve (broken line) superimposed by the 35 kV molybdenum emission line (continuous line).

2.10.2 Geometry of Diffraction

A crystal lattice can be considered as a family of planes extending through the atoms of the lattice and defined by a triplet (*hkl*) of whole numbers, which are called MILLER INDICES. The incident waves are assumed to be reflected by these planes. Tbe spacing $d_{(hkl)}$ between adjacent planes with Miller indices (*hkl*) can be calculated from the angle 2θ using the BRAGG equation:

$$n\lambda = 2\, d_{(hkl)} \sin\theta \qquad (2.19)$$

where n is an integer 0, 1, 2, 3, ..., called the order, λ is the X-ray wavelength, $d_{(hkl)}$ is the distance between adjacent planes in the crystal, θ is one-half the angle of deviation of the diffracted rays from the incident X-rays[16].

The geometry of the diffraction of X-rays in a crystal is given in Figure 2.18.

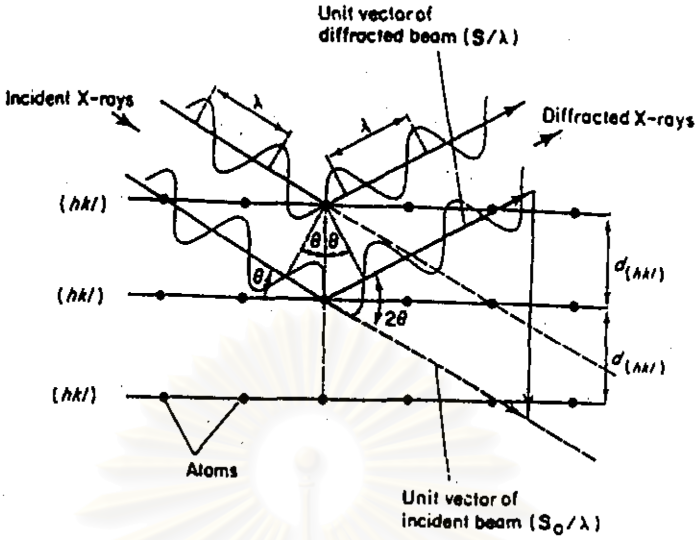

Figure 2.18 Geometry of the diffraction of X-rays in a crystal

2.10.3 X-ray Diffractometer

An X-ray diffractometer (X-ray spectrometer) (Figure 2.19) is built of the following parts[16]:

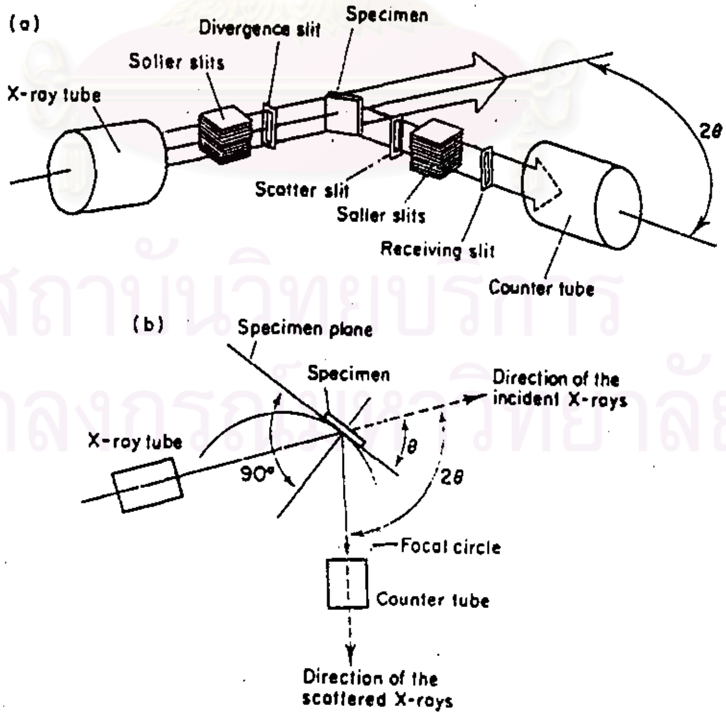

Figure 2.19 (a) schematic representation of an X-ray diffractometer. (b) Geometry of an X-ray diffractometer.

2.10.4 Measurement of the Degree of Crystallinity in Polymers by X-ray Diffraction Analysis

The degree of crystallinity can be determined if the crystalline and amorphous scattering in the diffraction pattern can be separated from each other.

The degree of crystallinity (χ_c) is equal to the ratio of the integrated crystalline scattering to the total scattering, both crystalline and amorphous, and is given by:

$$\chi_c = \int_0^{\infty} s^2 I_c(s)ds \;/\; \int_0^{\infty} s^2 I(s)ds \qquad (2.20)$$

where s is the magnitude of the reciprocal-lattice vector and is given by

$$s = (2\sin\theta)/\lambda \qquad (2.21)$$

θ is one-half the angle of deviation of the diffracted rays from the incident X-rays, λ is the X-ray wavelength, $I(s)$ is the intensity of coherent X-ray scatter from a specimen (both crystalline and amorphous), $I_c(s)$ is the intensity of coherent X-ray scatter from the crystalline region[16,17].

The degree of crystallinity calculated from eq. 2.20 tends to be smaller than the true crystalline fraction, because part of the X-ray intensity that is scattered by the crystalline region is lost from the peaks and appears as diffuse scatter in the background as a result of atomic thermal vibrations and lattice imperfections[16].

Differentiation between crystalline and amorphous scattering in coherent scattering is very difficult, and sometimes provides errors which seriously influence the measurement of the degree of crystallinity. There are two basic methods for differentiation between crystalline and amorphous scattering:

(i) For samples where completely amorphous or completely crystalline specimens cannot be obtained. In this case (Figure 2.20) a line is drawn, which should connect the minima between the crystalline peaks. The scatter intensity above this line (I_c) is from a crystalline region, whereas the scatter intensity below this line (I_a) is from an amorphous region. The degree of crystallinity (χ_c) can then be calculated from eq. (2.20)[16].

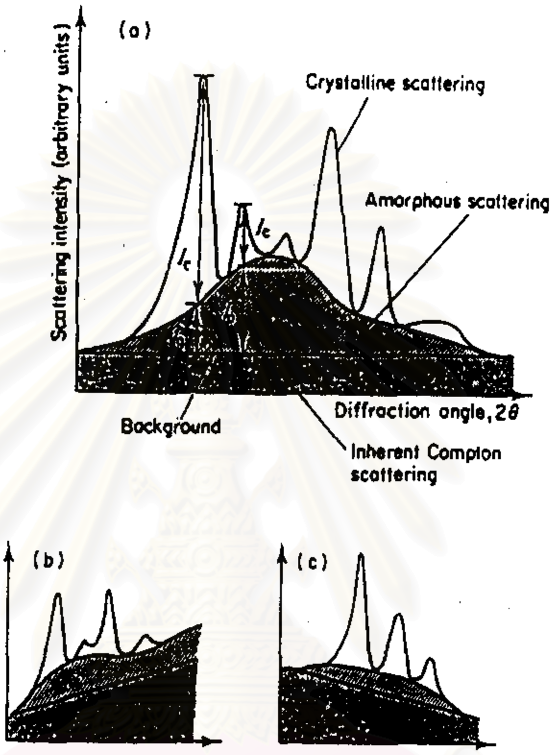

Figure 2.20 Differentiation between crystalline and amorphous scattering for different semicrystalline polymer samples: (a), (b), and (c) show different positions of back ground lines.

(ii) For samples where completely amorphous or completely crystalline specimens can be obtained. In this case (Figure 2.21),

(a) an amorphous reference specimen,

(b) a crystalline reference specimen, and

(c) a specimen of unknown crystallinity

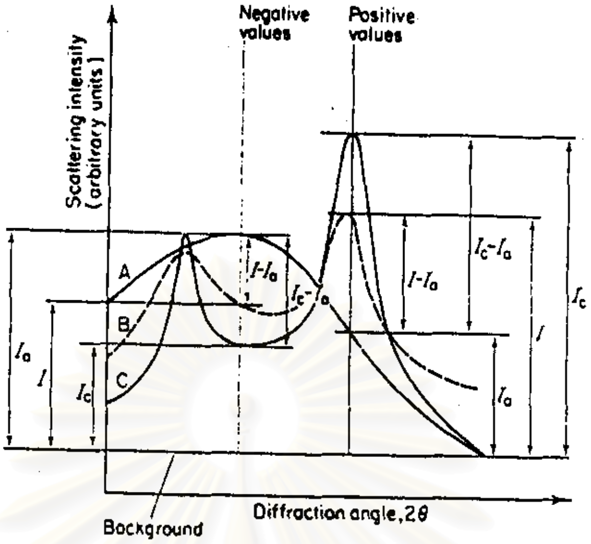

Figure 2.21 Diffraction intensity curves for: A, amorphous; B, unknown, and C, crystalline specimens.

are examined separately. The degree of crystallinity (χ_c) can then be calculated from

$$\chi_c = \frac{(I-I_a)_i - K}{(I_c-I_a)_i} \tag{2.22}$$

where I is the scatter intensity from an unknown sample, I_a is the scatter intensity from an amorphous reference specimen, I_c is the scatter intensity from a crystalline reference specimen, K is a constant which can be calculated from the slope of a curve obtained by plotting $I-I_a$ versus I_c-I_a (Figure 2.22)[16].

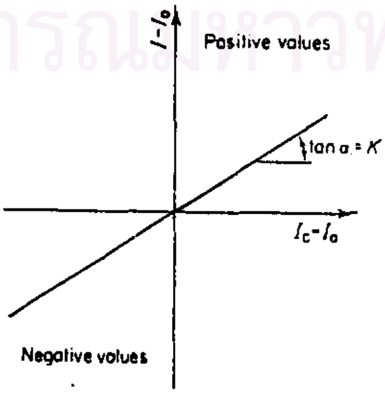

Figure 2.22 Plot of scattering intensity differences obtained from Figure 2.21.

2.11 Literature Reviews

Pattanakul, et al. [1] studied the effect of virgin, high-density polyethylene (HDPE) / recycled HDPE composition on the physical properties of the blends. The recycled HDPE was obtained from a post consumer cycle of milk bottles. It was found that elongation at break was the mechanical property mostly affected by the content of recycled HDPE. However, the recycled HDPE from milk bottles was found to be a material of useful properties not largely different from those of virgin resins and thus could be used, at an appropriate concentration in virgin HDPE, for different applications.

Kartalis et al. [2] studied a remelting-restabilization technique that was applied for the recycling of postused, yellow-pigmented HDPE bottle creates. Multiple extrusion cycle procedure, at different reprocessing temperatures, was performed for monitoring the processing stability of the restablilized and nonrestabilized material as reference. In addition, mechanical property measurements were carried out to study further the effect of restabilization on the performance used to investigate the role of new pigments on the final recycled product. The results illustrate that restabilization of postused crates leads to careful reprocessing without severe degradation, which is an essential prerequisite for reuse in the original application.

Herbert et al. [3] studied the properties of blown film made from post-consumer recycled materials. Post-consumer recycled LLDPE film was blended with a virgin LLDPE resin at several levels in a twin-screw extruder, and the melt index, storage modulus, and loss modulus of these blends were measured. Using these blends, blown film experiments were performed according to a factorial design, and the films produced were tested for dart drop impact strength, cross and machine direction tear strength, and gauge uniformity.

Butler et al. [13] studied the blown film process, a complex manufacturing process, in which film properties are found to be greatly influenced by the fabrication variables from which the film was produced. It focussed on the control of these variables to demonstrate the methods of process control used for optimization of film properties for a linear low-density polyethylene (LLDPE). The influences of crystallinity and orientation of polymer molecules must be correlated to fabrication variables to provide insight as to why the film properties vary. The fundamental understanding of crystallization of polyethylene requires the analysis of several factors that influence the quenching of the blown film bubble. The crystallinity effects must be determined before orientation effects can be accurately evaluated. When the crystallinity effects are included, the orientation effects can then be predicted. A designed experiment technique was used to correlate film properties to fabrication variables. By combining the film property studied, the fundamental characterization of crystallinity and orientation with correlation to key fabrication variables has provided insight into understanding and predicting performance of the blown film process.

Viksne et al. [23] investigated the correlation between mechanical and rheological properties of LDPE waste and LDPE/HDPE waste blends with different degrees of degradation. To predict the suitability of PE wastes for a blown-film extrusion process, parameters such as melt flow index, morphology of the extrudate's surface, and melt elongation at break were determined. For the binary blends of LDPE/HDPE waste, the melt flow index ratio of the components was also used. The blown-film extrusion of this PE waste is possible only within the defined critical values of these parameters.

Fruitwala et al. [24] used wide a angle X-ray analysis (WAX), and transmission electron microscopy (TEM) to evaluate the molecular orientation of two polyolefin films in three principal planes. It was shown that X-ray analysis can be valuable in the development of new resins.

Kim et al. [25] prepared the blown film HDPE with unimodal and bimodal molecular weight distribution under several processing conditions, and their morphologies were extensively characterized. The high molecular weight tail (MW > ~10^6) of the molecular weight distribution seems to play a critical role on the morphology of blown HDPE films irrespective of the molecular weight distribution mode of the resins. As the content of high molecular weight species increased, the network structure of lamellar stacks was then better developed. The intercrystalline connectivity along the normal direction of lamellar stacks was higher than that along the transverse direction of lamellar stacks.

Kim et al. [26] prepared blown films having a broad range of morphologies from HDPE with unimodal and bimodal molecular weight distribution under several processing conditions. The effects of their morphological features on the dart drop impact resistance, Elmendorf tear strength, and tensile properties of films were characterized. The organization of lamellar stacks seems to play a critical role on the mechanical properties of the blown HDPE films. The dart drop impact resistance of the blown HDPE films is highly dependent on the presence of the network structure of lamellar stacks and the level of the intraconnectivity and interconnectivity of lamellar stacks. The coherent orientation of lamellar stacks leads to significant anisotropy of tear and tensile properties.

Gibbs [27] evaluated whether post-consumer recycled high-density polyethylene (HDPE) can be used or modified to take full advantage of its potential to produce a quality part, specifically, in the blow moulding of monolayer containers. Commercial recycled HDPE resins are assessed, and suggestions are given on how to improve these resins and the recycling process.

Vaccaro [28] studied the polymer waste recycling of several different polyolefins, such as, polyethylene, polypropylene, and polystyrene by compatibilization of low-density polyethylene (LDPE) with polypropylene (PP) through the addition of maleated polyethylene and maleated polypropylene. Prediction of the tensile properties of these blends is attempted, using a model based on the continuity of phases in a two-component mixture of thermoplastics.

Kim et al. [29] prepared and investigated the biaxially oriented films of blends of HDPE with PP homopolymer and PP copolymers by a twin-screw extrusion and a lab-stretcher. Their properties were achieved by scanning electron microscopy (SEM), polarized microscopy, differential-scanning calorimeter, and universal testing machine. Three different kinds of PP copolymers were used: (i) random copolymer; (ii) ethylene-propylene (EP) block copolymer; (iii) ethylene-propylene-butylene (EPB) terpolymer. In the SEM study of the morphology of films of HDPE with various PP blends, phase separation was observed between the PP phase and the HDPE phase for all blends and compositions. In all blends, HDPE served to reduce the average spherulites size, probably acting as a nucleating agent for PP. The reduction of spherulite size appeared most significantly in the blend of EPB terpolymer and HDPE. A large increase of crystallization temperature was found in the blend of EPB terpolymer and HDPE, the improvement of tensile strength and modulus was observed with an increase of HDPE in reducing average spherulite size.

Darras et al. [35] studied tensile yield stress measurements have been performed on a series of four ethylene/1-butene copolymers covering the crystallintity range of 0.33-0.74. Samples were prepared from melt-crystallization and from solution-crystallization at various concentrations in decalin in order to span a wide range of crystal thickness. It is shown that tensile yield stress depends on crystal thickness rather than on crystallinity. This result is perfectly consistent with a plasticity model based on the nucleation of dislocations.

Gerrits et al. [36] studied the crystal orientation of solid-state biaxially drawn solution-crystallized ultra-high-molecular weight polyethylene (UHMW-PE) film, which was revealed from flat-plate wide-angle x-ray scattering (WAXS) patterns and interpreted in terms of crystal plasticity. A slightly drawn film ($\lambda \leq 3 \times 3$) possesses only a (100) planar orientation, whereas in a highly drawn film ($\lambda \leq 6 \times 6$), a mixed (100) and (110) planes, resulting in a (100) texture in a similar way to crystal deformation in uniaxially drawn polyethylene and by (110) $<1\bar{1}0>$ transverse slip and/or (310) twinning which results in a (110) texture. It is postulated that during transverse slip or twinning, the molecules deform without chain extension. As a consequence, neither the molecular draw ratio nor the tensile properties change significantly for macroscopically drawn ratios of above 10 in contrast to the data obtained for uniaxially drawn polyethylene.